IEEE Access
Multidisciplinary | Rapid Review | Open Access Journal

Received 18 January 2023, accepted 10 March 2023, date of publication 17 March 2023, date of current version 22 March 2023.

Digital Object Identifier 10.1109/ACCESS.2023.3258698

RESEARCH ARTICLE

Underwater Image Enhancement Based on Adaptive Color Correction and Improved Retinex Algorithm

SHIJIE LIN, ZHE LI, FUHAI ZHENG, QI ZHAO, AND SHIMENG LI
School of Mathematics and Statistics, Changchun University of Science and Technology, Changchun 130022, China

Corresponding author: Zhe Li (zheli200809@163.com)

This work was supported in part by the National Natural Science Foundation of China under Grant 12171054, and in part by the National Innovation Training Program for College Students under Grant 202210186041.

ABSTRACT In order to solve the problems about color distortion and low contrast of underwater images, we propose an underwater image enhancement algorithm that combines adaptive color correction with improved Retinex algorithm. Our algorithm is a single-image enhancement method that does not require specialized hardware and underwater scenes prior. Firstly, the adaptive color correction is carried out on the underwater distorted images to solve the color cast problem effectively. Then, on the one hand, we use the image decomposition to strengthen the detail part and obtain a detail enhanced image. On the other hand, we use the improved Retinex algorithm to strengthen the edge part and obtain an edge enhanced image. Finally, the detail enhanced image and the edge enhanced image are fused based on the non-subsampled shearlet transform (NSST) to obtain the final enhanced underwater image. The results show that our method outperforms several state-of-the-art methods about underwater image enhancement in terms of PCQI, UCIQE, UIQM and IE. By scale invariant feature transform (SIFT) algorithm, we calculate the number of feature matching points of the input image and the enhanced image, and our proposed method achieves the best experimental results. The source code of our proposed algorithm is available at: https://github.com/lin9393/ underwater-image-enhance.

INDEX TERMS Underwater image enhancement, adaptive color correction, improved Retinex algorithm, non-subsampled shearlet transform.

I. INTRODUCTION

With the increasing shortage of resources on land, the ocean that is rich in oil and mineral resources has been eagerly explored. Obtaining high-quality and clear underwater images is an important guarantee for the development of underwater vehicle control [1], underwater infrastructure inspection [2], marine biological research [3]. Therefore, enhancing the visual effects of underwater images is an important link of the ocean exploration journey. However, due to the attenuation and scattering of light in water, problems such as color cast, image blurring, and low contrast, will appear in underwater images [4]. In order to promote the subsequent research and application, it is necessary to enhance underwater image. Due to the diversity of water bodies and the inconsistency of image degradation, the expression forms of images are varied. Therefore, how to use image enhancement technology to extract underwater image information and solve various degradation problems is worth further study.

In recent years, underwater image enhancement has achieved significant progress by taking advantage of physical model-based methods, non-physical model-based methods and deep learning-based methods. In the following, we briefly review these relevant methods.

A. PHYSICAL MODEL-BASED METHODS

These methods in [5], [6], [7], [8], [9], [10], [11], and [12] establish underwater image enhancement models by studying

The associate editor coordinating the review of this manuscript and approving it for publication was Sudhakar Radhakrishnan.

the distortion principle of underwater images. He et al. [5] estimated the light composition and transmittance of underwater images through the dark channel prior principle. Indeed, the prior transmittance estimated in [5] is too large, which makes the final enhanced image dark. Shafuda et al. [6] combined light and dark priors to estimate backscattered light in underwater images. For the light absorption problem, Peng et al. [7] proposed a depth estimation method to accurately estimate the underwater scene depth. Yang et al. [8] introduced a novel background light estimation method which uses deep learning to capture red channel information of the background light in the dark channel. Gong et al. [9] improved the exposure of underwater images by fusing the polarization image with the intensity image. By estimating ambient light, Ueki [10] proposed a generalized dark channel prior model which can adapt to more underwater images. Considering the forward scattering, Park et al. [11] drew the conclusion that the distance of the observed object is inversely proportional to the geodesic color distance of the background light. Based on dark channel and underwater attenuation priors, Song et al. [12] enhanced underwater images by estimating the transmission map and background light. In short, physical model-based methods often require higher accurate estimation of complex underwater image parameters, which will cause the models to be sensitive to image types.

B. NON-PHYSICAL MODEL-BASED METHODS

These methods [13], [14], [15], [16], [17], [18], [19], [20], [21] utilize traditional image processing techniques to enhance underwater images. Ghani [13] used homomorphic filtering to remove blue-green noise and enhance image details. The methods proposed in [13] improved underwater image visibility by recursively overlapping contrast limited histograms and dual-image wavelet. Ancuti et al. [14] conducted multi-scale fusion to obtain enhanced images by introducing the white balance technique that can compensate the colors of underwater images and effectively improve the color authenticity. Chang et al. [15] proposed an adaptive color correction method combined with guided filtering, which improves the visual effect of underwater images to a certain extent. Based on channel priors and histogram equalization, Srinivas et al. [16] used the multi-scale Retinex technique to obtain the luminance component. Zhang [17] enhanced underwater images through the principle of minimum color loss and local adaptive contrast. On the basis of the Retinex algorithm, Zhang [18] obtained the detail enhanced images by fusing the Rayleigh distribution, adaptive gamma correction and differential pyramid techniques. Apart from that, histogram stretching [19], image layer separation [20] and swarm intelligence [21] are also adopted to improve brightness and contrast of underwater images. Non-physical model-based methods aim to modify image pixel values to improve visual quality. However, these methods ignore the underwater imaging mechanism, which induces that non-physical model-based methods have poor generalization ability.

C. DEEP LEARNING-BASED METHODS

Due to the powerful learning ability of deep learning, deep learning-based methods [22], [23], [24], [25], [26], [27] have achieved an unqualified success in the aspect of underwater image enhancement. However, these methods typically require a large amount of data to build a dataset for training. Li et al. [22] transformed aerial images into underwater images by using the style classifier and conditional vector, which alleviates the problem of lack of real underwater images. The model proposed by Liu et al. [23] enhances underwater images by residual learning combined with polynomial loss function. A novel spiral generative adversarial framework introduced by Han et al. [24] can enhance image details while removing noise caused by scattering and attenuation. In order to learn underwater image feature, Li et al. [25] built the UIEB dataset that covers a wide range of underwater scenes and degradation forms. Based on a normalization method across space and channel dimensions, Fu et al. [26] devised the SCNet for learning underwater desensitized representation which is suitable for different water bodies, but the detail textures of the enhanced images are blurred. Li [27] designed a multi-color space embedded network which can effectively improve the visual quality of underwater images. Above all, deep learning-based methods rely on a large number of distorted and clear underwater images. However, most images are artificially synthesized which are different from the real-world underwater images, so the robustness and generalization ability of deep learning-based methods is limited.

In this paper, we pay attention to the problem about weak generalization ability of non-physical model-based methods, Inspired by the work in [14], we introduce an adaptive underwater image enhancement method that is suitable for underwater complex images. More precisely, our main contributions can be summarized as follows:

- We use color correction, contrast enhancement, tone adjustment and image fusion methods to achieve underwater image enhancement. Compared with contrast algorithms, our proposed algorithm has achieved better results on PCQI, UCIQE, UIQM and IE metrics.
- For the complex underwater environment, we propose an adaptive color correction method, which can remove the color cast of underwater images.
- We improve the Retinex algorithm to adaptively adjust the tone of underwater images, which can convert dark or bright underwater images into pleasing images.

The outline of the paper is organized as follows. Section II presents our proposed underwater image enhancement method. Section III presents the experimental results and several concluding remarks are provided in Section IV.

II. PROPOSED METHOD

In this paper, we firstly perform the adaptive color correction method on underwater distorted images in order to deal with the color bias phenomenon. Then on the one hand, the dual-scale image decomposition and Gamma correction are used

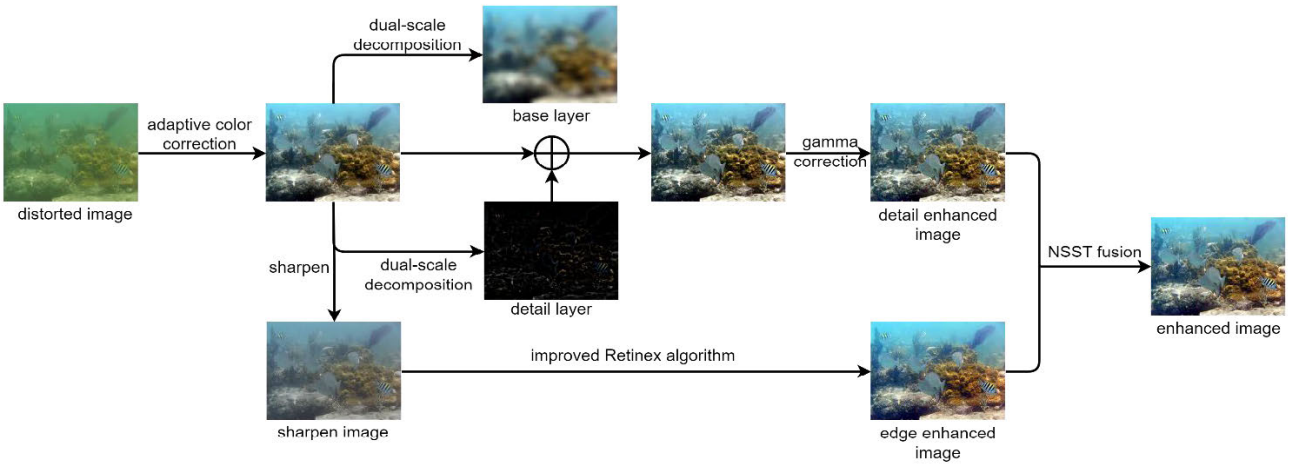

FIGURE 1. The flowchart of the proposed algorithm.

to yield a detail enhanced image. On the other hand, the sharpen algorithm and the improved Retinex algorithm are used to adjust the hue of the image to produce an edge enhanced image. Finally, based on NSST technique, we fuse the detail enhanced image and the edge enhanced image to obtain the final enhanced underwater image. The algorithm flow is shown in Figure 1.

A. ADAPTIVE COLOR CORRECTION

In order to effectively remove color cast, we propose an adaptive color correction method that consists of two parts, namely, the channel compensation and the color balance.

The color compensation theory proposed by Ancuti et al. [14] only compensates the red channel with constant compensation coefficients, which contradicts the complex underwater environment. As a consequence, we design a channel compensation method to restore the authenticity of underwater image color from a more comprehensive perspective.

Let $\overline{I_r}$, $\overline{I_g}$ and $\overline{I_b}$ respectively denote the average pixels of the red, green and blue channels. Since the green channel is often better preserved [14], if

$$\frac{\overline{I_r} + \overline{I_b}}{\overline{I_r} + \overline{I_b} + \overline{I_g}} < \frac{1}{3} \tag{1}$$

holds, then the red and blue channels are severely lost. Therefore, the color cast can be removed through color balance without the need for the channel compensation. If the inequality (1) does not hold, then it is necessary to perform channel compensation on the distorted images.

The complex underwater environment often makes the color distortion inconsistent. Therefore, it should separately compensate the red, green and blue channels, namely,

$$I_r(x) = I_r(x) + \alpha(\overline{I_g} - \overline{I_r})(1 - I_r(x))I_g(x), \tag{2}$$

$$I_g(x) = I_g(x) + \beta(|\overline{I_g} - \overline{I_b}|)(1 - I_g(x))I_b(x), \tag{3}$$

$$I_b(x) = I_b(x) + \gamma(|\overline{I_g} - \overline{I_b}|)(1 - I_b(x))I_g(x), \tag{4}$$

where $I_r(x)$, $I_g(x)$, and $I_b(x)$ respectively represent the pixel values of the red, green, and blue channels, α, β and γ are respectively compensation coefficients of red, green and blue channels. The following describes the calculation method of compensation coefficients in four cases. Let ε be an parameter that measures channel loss levels. If ε is too small, it will lead to over-compensation. If ε is too large, it will lead to under-compensation. The experiment shows that when $\varepsilon = 0.1$, it can balance the difference of loss level among channels well.

a. If $|\overline{I_g} - \overline{I_b}| \leq \varepsilon$, then

$$\alpha = 1 - ln(\overline{I_g} - \overline{I_r}), \beta = 0, \gamma = 0. \tag{5}$$

In this case, the loss of the blue and green channels is small, so we only need to compensate for the red channel.

b. If $\overline{I_b} - \overline{I_g} > \varepsilon$, then

$$\alpha = 1 - ln(\overline{I_g} - \overline{I_r}), \beta = 0, \gamma = -ln(\overline{I_b} - \overline{I_g}). \tag{6}$$

In this case, the image is bluish, indicating that the red and green channels are seriously lost, while the blue channel is well preserved. Hence we only compensate for the red and green channels.

c. If $\overline{I_g} - \overline{I_b} > \varepsilon$ and $\overline{I_r} - \overline{I_b} \leq \varepsilon$, then

$$\alpha = 1 - ln(\overline{I_g} - \overline{I_r}), \beta = (1 - ln(\overline{I_g} - \overline{I_r}))^{-1}, \gamma = 0. \tag{7}$$

In this case, the image is greenish, then we only compensate for the red and green channels. Notice that we refer to the color compensation method proposed in [15]. we impose the reasonable restrictions on the blue compensation to prevent the blue compensation from exceeding the red compensation.

d. If $\overline{I_g} - \overline{I_b} > \varepsilon$ and $\overline{I_r} - \overline{I_b} > \varepsilon$, then

$$\alpha = 0, \beta = 1 - ln(\overline{I_g} - \overline{I_b}), \gamma = 0. \tag{8}$$

In this case, the image is yellowish which illustrates that the blue channel is seriously lost while the red and green channels are well preserved, so we only compensate for the blue channel.

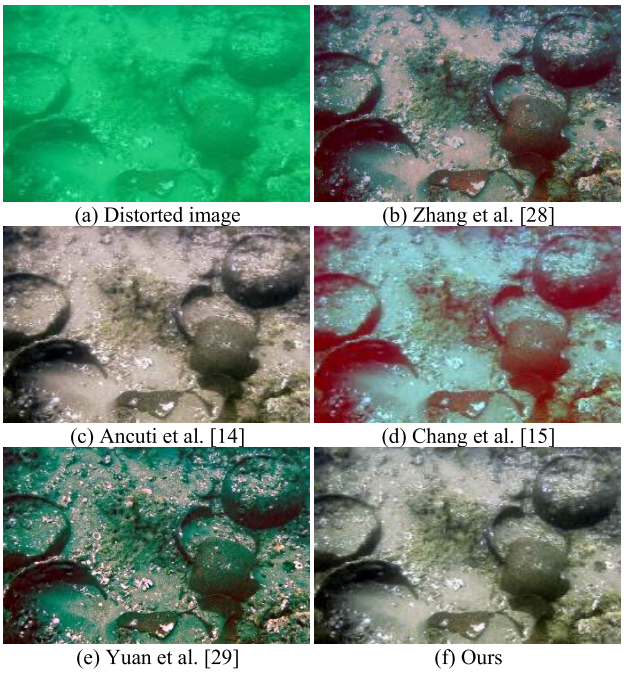

FIGURE 2. Color correction comparisons of different algorithms.

After obtaining the compensated image, we perform the color balance operation to adjust the image global tone. For $C \in \{R, G, B\}$, let $\overline{I_C}$ denote the mean value of the compensated image in C channel, then define

$$\begin{aligned} q_{c,1} &= 0.005 \frac{\max\{\overline{I_r}, \overline{I_g}, \overline{I_b}\}}{\overline{I_c}}, \\ q_{c,2} &= 1 - q_{c,1}. \end{aligned} \tag{9}$$

Let $Q(q_{c,1})$ and $Q(q_{c,2})$ denote the q_1 and q_2 quantile pixel values of the image in C channel, then we perform the following operation

$$I_c(x) = \begin{cases} Q(q_{c,1}) \ , I_c(x) < Q(q_{c,1}) \\ Q(q_{c,2}), I_c(x) > Q(q_{c,2}) \\ I_c(x), \text{others}. \end{cases} \quad , C \in \{R, G, B\} \tag{10}$$

to obtain the image $I_c(x)$. Finally, we stretch the image $I_c(x)$ to obtain the color corrected image, namely,

$$I_c = \frac{I_c - I_{c,\min}}{I_{c,\max} - I_{c,\min}}, \tag{11}$$

where $I_{c,\max}$ and $I_{c,\min}$ respectively represent the maximum and minimum values in C channel. Accordingly, we obtain the color corrected image I.

Figure 2 shows the enhanced images by our proposed adaptive color correction method, and the color correction methods proposed by Zhang [28], Ancuti [14], Chang [15], Yuan [29]. Apparently, our color correction algorithm can effectively restore color fidelity and improve visual effects.

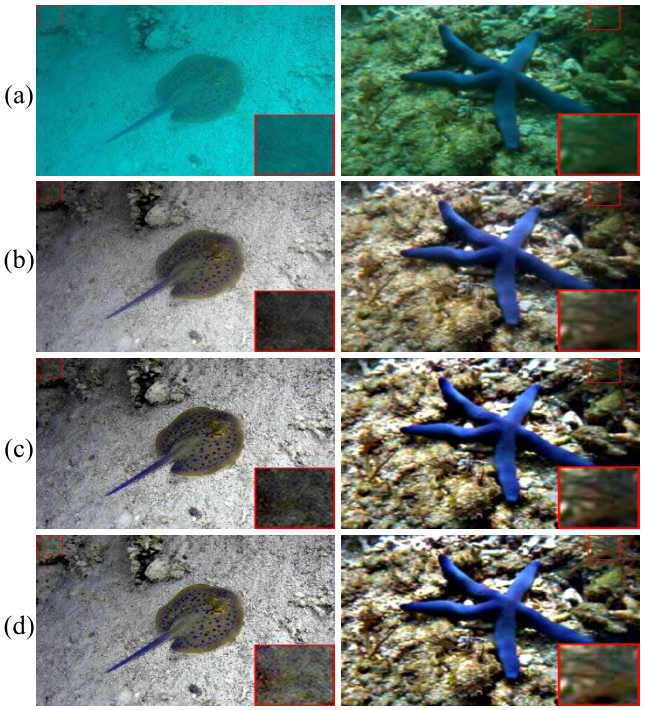

FIGURE 3. Visual comparisons of the different stages of distorted image enhancement. (a) distorted images (b) the images after adaptive color correction (c) the images after dual-scale decomposition (d) the images after gamma correction.

B. DUAL-SCALE DECOMPOSITION AND GAMMA CORRECTION

Although the color correction method can well solve the color bias problem, the detail texture of color corrected image is not rich enough. Consequently, it is necessary to enhance the contrast of underwater image. In particular, we utilize dual-scale image decomposition to enhance the details of underwater images. That is to say, we use the large-scale mean filtering to decompose the color corrected image I into two parts: the base layer C_n and detail layer D_n, namely,

$$\begin{cases} C_n = I \otimes Z, \\ D_n = I - C_n, \end{cases} \tag{12}$$

where $\otimes$ is the convolution operation and Z is the mean filtering with size 50*50. To prevent insufficient image detail extraction or excessive image smoothing, the dual-scale detail enhanced image is computed by,

$$R_{out} = I + \zeta D_n, \tag{13}$$

where ζ is the enhancement coefficient. Finally, applying Gamma correction [30] to the image R_{out} yields the detail enhanced image I_D.

Figure 3 shows an example of visual enhancement effect at the different stages of a distorted image. From Figure 3, we can observe that the image details are improved after dual-scale enhancement. After gamma correction, the local image brightness is adjusted. Apparently, the final detail enhancement images appear more beautiful.

C. IMPROVED RETINEX ALGORITHM

By the sharpen method proposed in [14], we strengthen the edge of the color corrected image I to get the sharpen image I_S. Concretely, let G be Gaussian filtering, and $\psi\{.\}$ be normalized operator, then I_S is computed by

$$I_S = (I + \psi\{I - G \otimes I\})/2. \tag{14}$$

However, I_S tends to appear too bright or dim. Thus we design an improved Retinex algorithm for underwater image tone adjustment. Basically, the improved Retinex algorithm is divided into three parts: global adaptation, local adaptation and color balance.

Firstly, global adaptation is carried out. According to the Weber-Fechner law, the brightness perception of human eyes is approximately a logarithmic function [31]. The brightness value of the estimated scene, denote by $L_w(x, y)$, is computed by,

$$L_w(\mathrm{x,y}) = 0.299 I_r(\mathrm{x,y}) + 0.587 I_g(x, y) + 0.114 I_b(x, y). \tag{15}$$

The brightness value after global adaptation, denote by $L_g(x, y)$, is computed by

$$L_g(x, y) = \frac{ln(L_w(x, y)/\overline{L_w} + 1)}{ln(L_{w,\max}/\overline{L_w} + 1)}, \tag{16}$$

where $L_{w,\max}$ is the maximum value of the estimated scene brightness value. Let $\overline{L_w}$ be the log-average brightness denoted by

$$\overline{L_w} = \exp\left(\frac{1}{N}\sum_{x,y} ln\left(\delta + L_w(x, y)\right)\right), \tag{17}$$

where N represents the total number of pixels and δ is a small positive number. The traditional Retinex algorithm uses Gaussian filtering to adjust the tone. However, in the area of high brightness, the estimated reflection components appear very dark, which will result in halo artifacts. Therefore, we use guided filtering [32] to replace the Gaussian filtering, namely

$$H_g(x, y) = Guide\left(L_g(x, y), g_{\max}(L_g(x, y))\right), \tag{18}$$

where *Guide* represents the guide filtering, g_{max} represents the maximum filtering.

Next, local adaptation is performed. The offset β that adaptively changes with scene content is computed by

$$\beta = \lambda\overline{L_g}, \tag{19}$$

where λ is the nonlinear control parameter and $\overline{L_g}$ is the global adaptive log-average brightness. The contrast enhancement factor $\alpha(x, y)$ is computed by

$$\alpha(x, y) = \left(1 + \eta\frac{L_g(x, y)}{L_{g,max}}\right)^{1+\frac{L_{g,max}}{L_{g,max}+\eta L_g(x,y)}}, \tag{20}$$

where $L_{g,max}$ is the maximum value of L_g. Consequently, the reflection component $R(x, y)$ is computed by

$$R(x, y) = \alpha(x, y) ln\left(\frac{L_g(x, y)}{H_g(x, y)} + \beta\right). \tag{21}$$

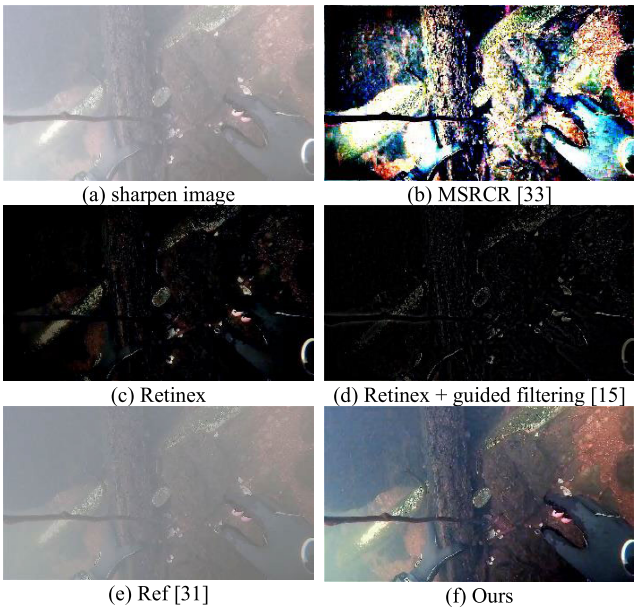

FIGURE 4. The comparisons of different tone adjustment algorithms.

Finally, we perform our proposed color balance operation defined by (9)-(11) on the image I_{out} by

$$I_{out}(\mathrm{x,y}) = \frac{R(x, y)}{L_w(x, y)} I_S \tag{22}$$

to obtain the edge enhanced image I_E.

Traditional Retinex algorithm often fails to get good results when processing high-brightness images, because the logarithmic processing of the reflection component compresses the display range of the bright area, which results in the weakening of image details. Inspired by the image tone restoration algorithm proposed in [31], we use the color balance technology to make the improve Retinex algorithm applicable to underwater image tone restoration, while adding maximum filtering to complement local adaptation. The contrast enhancement factor $\alpha(x, y)$ can effectively balance the logarithmization processing in the reflection component. Figure 4 compares our improved Retinex algorithm with several tone adjustment algorithms, including MSRCR [33] algorithm, traditional Retinex algorithm, the improved Retinex algorithm with guided filtering [15] and the method proposed in [31]. Figure 4 indicates that improved Retinex algorithm is more effective than the contrast algorithms in the aspect of adjusting the brightness of underwater images.

D. IMAGE FUSION

NSST is an advanced multi-scale geometric analysis tool with the characteristics of translation invariance and multi-directionality. An image can be decomposed by NSST to obtain low-frequency and high-frequency images [34]. We fuse the detail enhanced image I_D and edge enhanced image I_E, which are respectively labeled as Image A and Image B for convenience. We use the NSST to obtain the

Algorithm 1 Underwater Image Enhancement Based on Adaptive Color Correction and Improved Retinex Algorithm

1: **Input**: input image
2: **if** Eq. (1) holds **then**
3: Calculate compensation coefficients by Eqs. (5)-(8).
4: Compensates for red, green and blue channels by Eqs. (2)-(4).
5: **end if**
6: Perform the color balance operation by Eqs. (9)-(11).
7: Compute the detail enhanced image by Eqs. (12)-(13).
8: Compute the edge enhanced image by Eqs. (14)-(22) and Eqs. (9)-(11).
9: Perform NSST to obtain low-frequency and high-frequency of the detail enhanced image and the edge enhanced image.
10: Perform weighted fusion by Eqs. (23)-(26) for the low-frequency image.
11: Perform PAPCNN fusion for the high-frequency image.
12: Perform the inverse NSST to obtain the final enhanced image.
13: **Output** the final enhanced image

low-frequency and high-frequency components of Image A and Image B.

We compute the saliency weight and saturation weight to fuse the low frequency images. The saliency weight is intended to emphasize underwater images that lose saliency, but it tends to favor regions with high luminance values. Saturation weight can make full use of highly saturated regions to adapt chromaticity information.

The saliency weight W_S is computed by

$$W_S = (L - L_{mean})^2 + (a - a_{mean})^2 + (b - b_{mean})^2, \quad (23)$$

where L, a, b respectively represent the brightness layer, red-green layer, yellow-blue layer of the Lab image, and $L_{mean}, a_{mean}, b_{mean}$ respectively express the mean pixel value of the corresponding layer. The saturation weight W_{Sat} is computed by

$$W_{Sat} = \sqrt{1/3[(R - L)^2 + (G - L)^2 + (B - L)^2]}, \quad (24)$$

where R, G, B respectively represent the three channels of the RGB image.

Using saliency weights W_{S_k} and saturation weights W_{Sat_k} associated to Image A and Image B. we compute the aggregation maps W_k by

$$W_k = \frac{W_{S_k} + W_{Sat_k}}{W_{S_A} + W_{Sat_A} + W_{S_B} + W_{Sat_B}}, k \in \{A, B\}. \quad (25)$$

The low-frequency fused image I_{low} is computed by

$$I_{low} = W_A I_{low_A} + W_B I_{low_B}, \quad (26)$$

where I_{low_A}, I_{low_B} denote the low-frequency component of Image A and Image B respectively.

We use the parameter adaptation pulse coupled neural networks (PAPCNN) [34] for high frequency image fusion. PAPCNN can capture edges and details of high-frequency images only by iteration, instead of training. Finally, we perform the inverse NSST on the fused low-frequency and high-frequency images to get the final enhanced underwater image.

TABLE 1. The IE values of detail enhanced images, edge enhanced images and fused images for Figure 3.

	detail enhanced images	edge enhanced images	fused images
Fig. 3 Left	7.6722	7.7087	**7.7422**
Fig. 3 Right	7.5471	7.6409	**7.8381**

In order to illustrate the effectiveness of the fusion technique, we take the images in Figure 3 to compare the image information entropy (IE) values of detail enhanced images, edge enhanced images and fused images. As shown in Table 1, the IE value of the fused image is improved, After introducing the above sub-algorithms, the complete description of our proposed algorithm is exhibited in Algorithm 1.

III. EXPERIMENTS

A. EXPERIMENTAL SETUP

We conduct experiments on a 64-bit Windows 10 operating system with a running memory of 16G. All simulation results are calculated in the MATLAB (2019b) environment. In order to control the amount of calculation, the number of NSST decomposition layers is set to 2, the number of high-frequency images per layer is $[2^2, 2^3]$, the number of directions per layer is [6, 6]. The detail enhancement coefficient ζ is set to 0.5. Guide filtering parameters are set to $r = 10, eps = 0.09$.

In order to verify the effectiveness of our proposed algorithm, we selected blue, green, yellow and blurred underwater degraded images from the UIEB dataset. We compare our proposed algorithm with five state-of-the-art methods about underwater image enhancement, namely, IBLA (2017) [7], CBFU (2018) [14], NFSI (2019) [21], MBOT (2020) [12] and SCNet (2022) [26] subjective and objective Comparison.

B. SUBJECTIVE COMPARSION

Figure 5 contains the comparison results of 8 different underwater images enhanced by the above algorithms. These images can be divided into four groups that represent four situations of underwater images, namely, bluish (Img 1, 2), greenish (Img 3, 4, 5), yellowish (Img 6, 7) and hazy (Img 8) underwater images.

It can be seen from Figure 5 that the IBLA algorithm can't solve the degradation problems about image color well. Although the CBFU and NFSI algorithms can solve the problem about various color distortions, they can't enhance the image details and contrast well. In addition, the enhanced image is grayish, the color characteristics are not obvious. The MBOT and SCNet algorithms have good enhancement in image details and contrast, but they can't solve

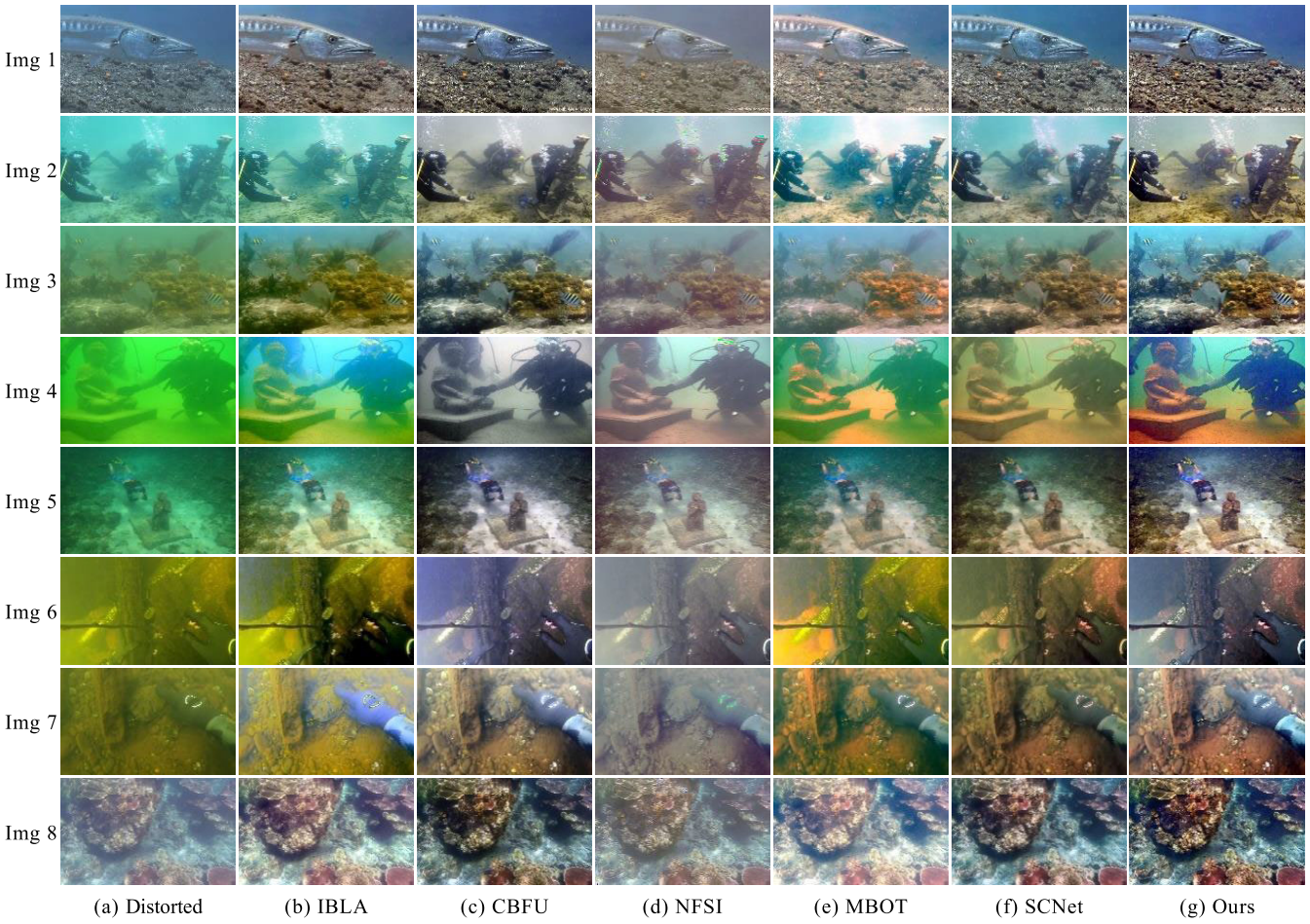

FIGURE 5. Subjective comparisons of different algorithms.

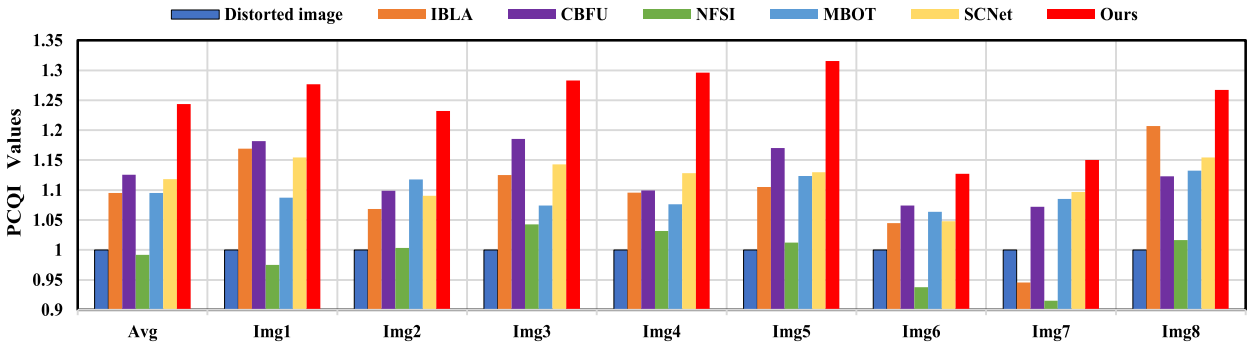

FIGURE 6. PCQI values of the enhanced images obtained by different algorithms.

the problem about color deviation when processing green and yellow images. In contrast, our proposed algorithm is suitable for the images in the different underwater environments, so our algorithm can solve different degradation problems, such as, color correction, noise elimination and detail preservation. In brief, our proposed algorithm can better improve the subjective visual effect of underwater images.

C. OBJECTIVE COMPARSION

In order to illustrate the effectiveness of our proposed algorithm objectively, PCQI [35], UCIQE [36], UIQM [37], and IE indexes are selected as the evaluation metrics of different algorithms. PCQI is used to compare the contrast difference between two images. A higher PCQI value suggests better visibility of the enhanced image. UCIQE reflects the chroma, saturation and contrast of underwater images. The higher

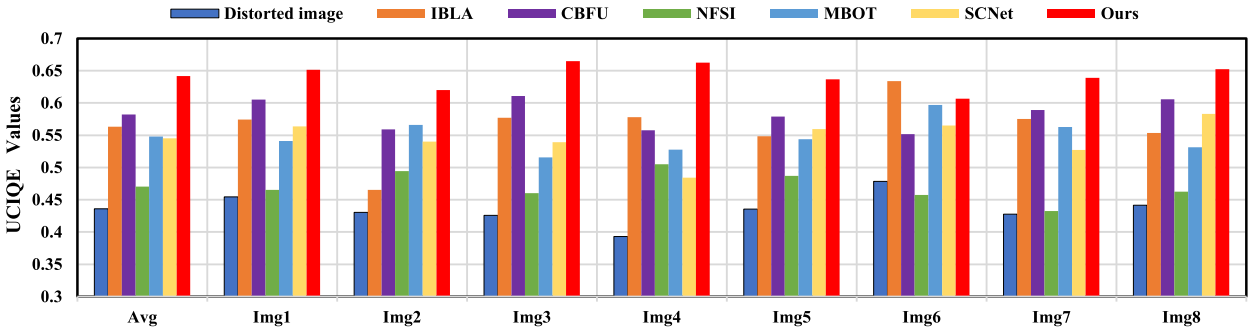

FIGURE 7. UCIQE values of the enhanced images obtained by different algorithms.

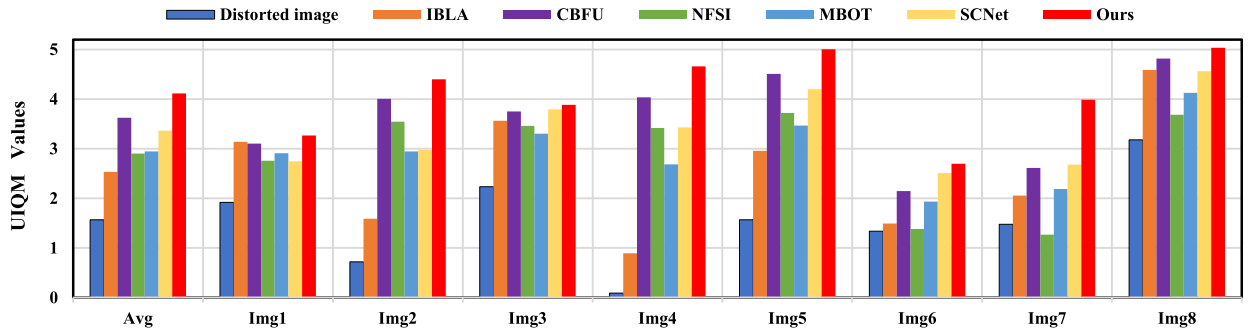

FIGURE 8. UIQM values of the enhanced images obtained by different algorithms.

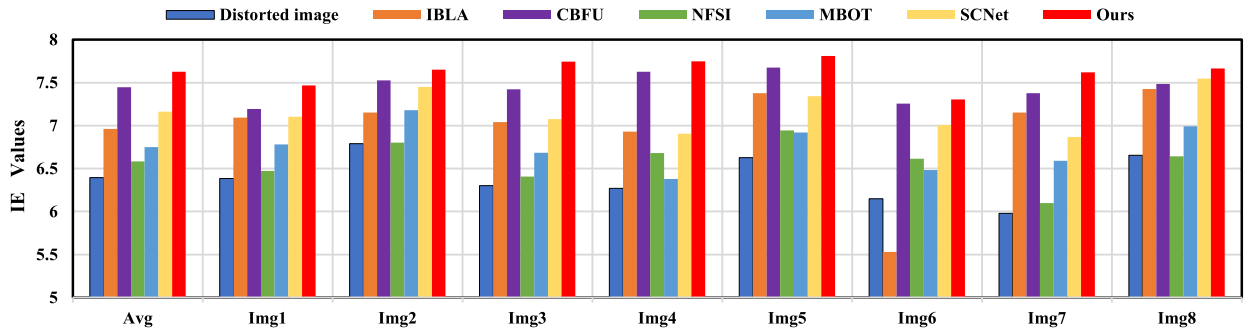

FIGURE 9. IE values of the enhanced images obtained by different algorithms.

TABLE 2. Quantitative comparisons of different methods on the UCCS [40] and UIEB [25] datasets.

Methods	UCCS [40]				UIEB [25]			
	PCQI↑	UCIQE↑	UIQM↑	IE↑	PCQI↑	UCIQE↑	UIQM↑	IE↑
Distorted image	-	0.4111	0.2352	6.2194	-	0.5196	1.9544	6.7863
IBLA [7]	1.1343	0.5011	1.7664	6.7469	1.0744	0.5990	2.9342	6.9327
CBFU [14]	1.1768	0.5424	3.8158	7.5318	1.0660	0.5923	3.7143	7.3866
NFSI [21]	1.0864	0.4961	3.2638	7.1759	0.9529	0.5347	3.5746	6.9823
MBOT [12]	1.1238	0.5357	2.7330	6.5291	1.0734	0.6158	2.8627	6.4994
SCNet [26]	1.0986	0.4989	2.8965	7.0845	1.0481	0.5902	3.3461	7.3746
Ours	**1.2592**	**0.5806**	**4.6694**	**7.6223**	**1.1871**	**0.6249**	**4.0392**	**7.5891**

the UCIQE value, the better the image quality. UIQM is closely related to human vision, which embodies the color, clarity and contrast of underwater images. A higher UIQM value means that the enhanced images are more consistent

TABLE 3. Ablation study on the UCCS [40] and UIEB [25] datasets.

Ablated models	UCCS [40]				UIEB [25]			
	PCQI↑	UCIQE↑	UIQM↑	IE↑	PCQI↑	UCIQE↑	UIQM↑	IE↑
Case1	1.1476	0.5631	4.0653	6.9991	1.1153	0.5895	3.4945	7.2371
Case2	1.1648	0.5686	4.4521	7.5841	1.0887	0.6110	3.9960	7.5385
Case3	1.2245	0.5843	4.2313	7.6860	1.1729	0.6300	3.9498	7.6086
Case0	1.2592	0.5806	4.6694	7.6223	1.1871	0.6249	4.0392	7.5891

TABLE 4. The average number of feature points about images in Figure 5.

Methods	Numbers↑
Distorted image	231.00
IBLA [7]	769.75
CBFU [14]	942.25
NFSI [21]	347.00
MBOT [12]	796.88
SCNet [26]	792.27
Ours	**1765.25**

with human visual perception. IE reflects the richness of image information. The higher the IE value, the more detailed information the enhanced image contains.

Figure 6-Figure 9 show PCQI, UCIQE, UIQM and IE values of different algorithms for the images in Figure 5. Notice that only the UCIQE value of Image 6 enhanced by our algorithm is slightly lower than the IBLA algorithm. However, the images enhanced by color of the IBLA algorithm have color distortion. The IBLA algorithm can not remove the yellow background. The reason is that the UCIQE index tends to evaluate the contrast of the image.

Indeed, even if there is color difference in the image, it is still possible to obtain a higher UCIQE value [38], [39]. Hence UCIQE index has certain limitations. In the other underwater environments, the PCQI, UCIQE, UIQM, and IE values of our proposed algorithm have achieved the best results. Overall, our proposed algorithm significantly enhanced in terms of color correction, image saturation and image contrast. The enhanced images are more consistent with the visual perception of human eyes.

Beyond that, the objective comparisons were conducted on the UCCS [40] and UIEB [25] datasets. The UCCS dataset contains 100 images in blue, blue-green and green, respectively. The UIEB dataset contains 890 images of various underwater scenes. The objective comparison results are shown in Table 2, from which we can see that our algorithm has achieved the best results on PCQI, UCIQE, UIQM and IE indexes on the UCCS and UIEB datasets.

D. ABLATION STUDY

To verify the effectiveness of our proposed model, we perform ablation experiments in the following cases. Case1 represents our model without adaptive color correction. Case2 represents our model without detail enhancement. Case3 represents our model without edge enhancement, and Case0 represents the results of our proposed model.

Table 3 shows the results of the ablation experiments on the UCCS and UIEB datasets. The best result is in red whereas the second best result is in blue. As presented in Table 3, our proposed model achieves the best performance in the two test datasets, which indicates that each key component contributes to the good performance of our method.

E. APPLICATION TEST

For many downstream tasks of underwater images, it is of great significance to compute matching point detection by SIFT algorithm [41]. The effectiveness of our proposed algorithm is verified by calculating the matching of feature points between the enhanced images and the original images. The greater the number of feature matching points, the more significant the local feature enhancement effect is.

Table 4 shows the results about the average feature points of the images in Figure 5. The average number of feature matching points in the original distorted image is 231. After enhanced by our algorithm, the average number of feature matching points is 1765.25, which has great advantage over other algorithms. Moreover, the images enhanced by our algorithm can have better detailed feature information.

IV. CONCLUSION

The complex underwater environment causes the problems about color distortion, low contrast and image blur. Aiming at these phenomena, we propose an underwater image enhancement algorithm based on adaptive color correction and improved Retinex algorithm. The designed adaptive color correction algorithm can effectively remove various color distortion. The improved Retinex algorithm can enhance the details and edges of the color corrected image. The detail enhanced image and the edge enhanced image are fused through NSST to produce the final enhanced image. The experimental results show that our proposed algorithm can effectively improve the visual effect of underwater distorted images in different underwater environments. Our proposed algorithm not only outperforms several existing algorithms in PCQI, UCIQE, UIQM, and IE indexes but also performs the best value on the SIFT application test. Although our proposed algorithm has achieved good results in enhancing visual effects of underwater images, image fusion using NSST requires a large amount of computation. To this end, we

consider exploring efficient algorithms suitable for underwater image fusion in our future work.

REFERENCES

[1] A. Sahoo, S. K. Dwivedy, and P. S. Robi, "Advancements in the field of autonomous underwater vehicle," *Ocean Eng.*, vol. 181, pp. 145–160, Jun. 2019, doi: 10.1016/j.oceaneng.2019.04.011.

[2] G. L. Foresti, "Visual inspection of sea bottom structures by an autonomous underwater vehicle," *IEEE Trans. Syst., Man, Cybern., B*, vol. 31, no. 5, pp. 691–705, Oct. 2001, doi: 10.1109/3477.956031.

[3] S. Mark, E. Harvey, and D. Abdo, "A review of underwater stereo-image measurement for marine biology and ecology applications," in *Oceanography and Marine Biology*. Boca Raton, FL, USA: CRC Press, 2016, pp. 269–304.

[4] Y. Wang, N. Li, Z. Li, Z. Gu, H. Zheng, B. Zheng, and M. Sun, "An imaging-inspired no-reference underwater color image quality assessment metric," *Comput. Elect. Eng.*, vol. 70, pp. 904–913, Aug. 2017.

[5] K. He, J. Sun, and X. Tang, "Single image haze removal using dark channel prior," *IEEE Trans. Pattern Anal. Mach. Intell.*, vol. 33, no. 12, pp. 2341–2353, Dec. 2011, doi: 10.1109/TPAMI.2010.168.

[6] F. Shafuda and H. Kondo, "A simple method for backscattered light estimation and image restoration in turbid water," in *Proc. OCEANS*, San Diego, CA, USA, Sep. 2021, pp. 1–6, doi: 10.23919/OCEANS44145.2021.9705704.

[7] Y.-T. Peng and P. C. Cosman, "Underwater image restoration based on image blurriness and light absorption," *IEEE Trans. Image Process.*, vol. 26, no. 4, pp. 1579–1594, Apr. 2017, doi: 10.1109/TIP.2017.2663846.

[8] S. Yang, Z. Chen, Z. Feng, and X. Ma, "Underwater image enhancement using scene depth-based adaptive background light estimation and dark channel prior algorithms," *IEEE Access*, vol. 7, pp. 165318–165327, 2019, doi: 10.1109/ACCESS.2019.2953463.

[9] K. Gong and D. Hua, "Research on the method of color compensation and underwater image restoration based on polarization characteristics," in *Proc. 3rd Int. Conf. Comput. Vis., Image Deep Learn. Int. Conf. Comput. Eng. Appl.*, Changchun, China, May 2022, pp. 746–751, doi: 10.1109/CVIDLICCEA56201.2022.9824370.

[10] Y. Ueki and M. Ikehara, "Underwater image enhancement based on the iteration of a generalization of dark channel prior," in *Proc. IEEE Vis. Commun. Image Process. (VCIP)*, Sydney, NSW, Australia, Dec. 2019, pp. 1–4, doi: 10.1109/VCIP47243.2019.8965726.

[11] E. Park and J.-Y. Sim, "Underwater image restoration using geodesic color distance and complete image formation model," *IEEE Access*, vol. 8, pp. 157918–157930, 2020, doi: 10.1109/ACCESS.2020.3019767.

[12] W. Song, Y. Wang, D. Huang, A. Liotta, and C. Perra, "Enhancement of underwater images with statistical model of background light and optimization of transmission map," *IEEE Trans. Broadcast.*, vol. 66, no. 1, pp. 153–169, Mar. 2020, doi: 10.1109/TBC.2019.2960942.

[13] A. S. A. Ghani, "Image contrast enhancement using an integration of recursive-overlapped contrast limited adaptive histogram specification and dual-image wavelet fusion for the high visibility of deep underwater image," *Ocean Eng.*, vol. 162, pp. 224–238, Aug. 2018, doi: 10.1016/j.oceaneng.2018.05.027.

[14] C. O. Ancuti, C. Ancuti, C. De Vleeschouwer, and P. Bekaert, "Color balance and fusion for underwater image enhancement," *IEEE Trans. Image Process.*, vol. 27, no. 1, pp. 379–393, Jan. 2018, doi: 10.1109/TIP.2017.2759252.

[15] J. Chang and X. Han, "Underwater image enhancement combining guided filtering and adaptive operators," *Comput. Eng. Appl.*, vol. 59, no. 4, pp. 216–223, 2023.

[16] S. Srinivas, V. R. Siddharth, S. Dutta, N. S. Khare, and L. Krishna, "Channel prior based Retinex model for underwater image enhancement," in *Proc. 2nd Int. Conf. Adv. Electr., Comput., Commun. Sustain. Technol. (ICAECT)*, Bhilai, India, Apr. 2022, pp. 1–10, doi: 10.1109/ICAECT54875.2022.9807919.

[17] W. Zhang, P. Zhuang, H.-H. Sun, G. Li, S. Kwong, and C. Li, "Underwater image enhancement via minimal color loss and locally adaptive contrast enhancement," *IEEE Trans. Image Process.*, vol. 31, pp. 3997–4010, 2022, doi: 10.1109/TIP.2022.3177129.

[18] W. Zhang, L. Dong, and W. Xu, "Retinex-inspired color correction and detail preserved fusion for underwater image enhancement," *Comput. Electron. Agricult.*, vol. 192, Jan. 2022, Art. no. 106585, doi: 10.1016/j.compag.2021.106585.

[19] W. L. Luo, S. Q. Duan, and J. W. Zheng, "Underwater image restoration and enhancement based on a fusion algorithm with color balance, contrast optimization, and histogram stretching," *IEEE Access*, vol. 9, pp. 31792–31804, 2021, doi: 10.1109/ACCESS.2021.3060947.

[20] C. Dai, M. Lin, J. Wang, and X. Hu, "Dual-purpose method for underwater and low-light image enhancement via image layer separation," *IEEE Access*, vol. 7, pp. 178685–178698, 2019, doi: 10.1109/ACCESS.2019.2958078.

[21] K. Z. M. Azmi, A. S. A. Ghani, Z. M. Yusof, and Z. Ibrahim, "Natural-based underwater image color enhancement through fusion of swarm-intelligence algorithm," *Appl. Soft Comput.*, vol. 85, Dec. 2019, Art. no. 105810, doi: 10.1016/j.asoc.2019.105810.

[22] N. Li, Z. Zheng, S. Zhang, Z. Yu, H. Zheng, and B. Zheng, "The synthesis of unpaired underwater images using a multistyle generative adversarial network," *IEEE Access*, vol. 6, pp. 54241–54257, 2018, doi: 10.1109/ACCESS.2018.2870854.

[23] P. Liu, G. Y. Wang, H. Qi, C. F. Zhang, H. Y. Zheng, and Z. B. Yu, "Underwater image enhancement with a deep residual framework," *IEEE Access*, vol. 7, pp. 94614–94629, 2019, doi: 10.1109/ACCESS.2019.2928976.

[24] R. Han, Y. Guan, Z. Yu, P. Liu, and H. Zheng, "Underwater image enhancement based on a spiral generative adversarial framework," *IEEE Access*, vol. 8, pp. 218838–218852, 2020, doi: 10.1109/ACCESS.2020.3041280.

[25] C. Li, C. Guo, W. Ren, R. Cong, J. Hou, S. Kwong, and D. Tao, "An underwater image enhancement benchmark dataset and beyond," *IEEE Trans. Image Process.*, vol. 29, pp. 4376–4389, 2019, doi: 10.1109/TIP.2019.2955241.

[26] Z. Fu, X. Lin, W. Wang, Y. Huang, and X. Ding, "Underwater image enhancement via learning water type desensitized representations," in *Proc. IEEE Int. Conf. Acoust., Speech Signal Process. (ICASSP)*, Singapore, May 2022, pp. 2764–2768, doi: 10.1109/ICASSP43922.2022.9747758.

[27] C. Li, S. Anwar, J. Hou, R. Cong, C. Guo, and W. Ren, "Underwater image enhancement via medium transmission-guided multi-color space embedding," *IEEE Trans. Image Process.*, vol. 30, pp. 4985–5000, 2021.

[28] W. Zhang, G. Li, and Z. Ying, "A new underwater image enhancing method via color correction and illumination adjustment," in *Proc. IEEE Vis. Commun. Image Process. (VCIP)*, St. Petersburg, FL, USA, Dec. 2017, pp. 1–4, doi: 10.1109/VCIP.2017.8305027.

[29] J. Yuan, Z. Cai, and W. Cao, "TEBCF: Real-world underwater image texture enhancement model based on blurriness and color fusion," *IEEE Trans. Geosci. Remote Sens.*, vol. 60, pp. 1–15, 2021, doi: 10.1109/TGRS.2021.3110575.

[30] Z. C. Liu, D. W. Wang, and Y. Liu, "Adaptive correction algorithm of uneven illumination image based on two-dimensional gamma function," *J. Beijing Univ. Technol.*, vol. 36, no. 2, pp. 191–196, 2016.

[31] H. Ahn, B. Keum, D. Kim, and H. S. Lee, "Adaptive local tone mapping based on Retinex for high dynamic range images," in *Proc. IEEE Int. Conf. Consum. Electron. (ICCE)*, Jan. 2013, pp. 153–156, doi: 10.1109/ICCE.2013.6486837.

[32] K. He, J. Sun, and X. Tang, "Guided image filtering," *IEEE Trans. Pattern Anal. Mach. Intell.*, vol. 35, no. 6, pp. 1397–1409, Jun. 2013, doi: 10.1109/TPAMI.2012.213.

[33] D. J. Jobson, Z.-U. Rahman, and G. A. Woodell, "A multiscale Retinex for bridging the gap between color images and the human observation of scenes," *IEEE Trans. Image Process.*, vol. 6, no. 7, pp. 965–976, Jul. 1997, doi: 10.1109/83.597272.

[34] M. Yin, X. Liu, Y. Liu, and X. Chen, "Medical image fusion with parameter-adaptive pulse coupled neural network in nonsubsampled shearlet transform domain," *IEEE Trans. Instrum. Meas.*, vol. 68, no. 1, pp. 49–64, Jan. 2019, doi: 10.1109/TIM.2018.2838778.

[35] S. Wang, K. Ma, H. Yeganeh, Z. Wang, and W. Lin, "A patch-structure representation method for quality assessment of contrast changed images," *IEEE Signal Process. Lett.*, vol. 22, no. 12, pp. 2387–2390, Dec. 2015, doi: 10.1109/LSP.2015.2487369.

[36] M. Yang and A. Sowmya, "An underwater color image quality evaluation metric," *IEEE Trans. Image Process.*, vol. 24, no. 12, pp. 6062–6071, Dec. 2015, doi: 10.1109/TIP.2015.2491020.

[37] K. Panetta, C. Gao, and S. Agaian, "Human-visual-system-inspired underwater image quality measures," *IEEE J. Ocean. Eng.*, vol. 41, no. 3, pp. 541–551, Jul. 2016, doi: 10.1109/JOE.2015.2469915.

[38] X. Chen, P. Zhang, L. Quan, C. Yi, and C. Lu, "Underwater image enhancement based on deep learning and image formation model," 2021, *arXiv:2101.00991*.

[39] Z. Jiang, Z. Li, S. Yang, X. Fan, and R. Liu, "Target oriented perceptual adversarial fusion network for underwater image enhancement," *IEEE Trans. Circuits Syst. Video Technol.*, vol. 32, no. 10, pp. 6584–6598, Oct. 2022, doi: 10.1109/TCSVT.2022.3174817.
[40] R. Liu, X. Fan, M. Zhu, M. Hou, and Z. Luo, "Real-world underwater enhancement: Challenges, benchmarks, and solutions under natural light," *IEEE Trans. Circuits Syst. Video Technol.*, vol. 30, no. 12, pp. 4861–4875, Dec. 2020, doi: 10.1109/TCSVT.2019.2963772.
[41] Y. Ke and R. Sukthankar, "PCA-SIFT: A more distinctive representation for local image descriptors," in *Proc. IEEE Comput. Soc. Conf. Comput. Vis. Pattern Recognit. (CVPR)*, Washington, DC, USA, 2004, pp. 506–513, doi: 10.1109/CVPR.2004.1315206.

SHIJIE LIN is currently pursuing the bachelor's degree with the School of Mathematics and Statistics, Changchun University of Science and Technology. He works on underwater image processing.

ZHE LI received the B.S. and M.S. degrees from the School of Mathematics and Statistics, Northeast Normal University, Changchun, China, in 2004 and 2006, respectively, and the Ph.D. degree from the School of Mathematics, Jilin University, Changchun, in 2011. She is currently a Professor with the School of Mathematics and Statistics, Changchun University of Technology, China. Her research interests include numerical approximate theory, verification computation, and signal processing.

FUHAI ZHENG is currently pursuing the bachelor's degree with the School of Mathematics and Statistics, Changchun University of Science and Technology. He works on underwater image processing.

QI ZHAO is currently pursuing the bachelor's degree with the School of Mathematics and Statistics, Changchun University of Science and Technology. She works on underwater image processing.

SHIMENG LI is currently pursuing the bachelor's degree with the School of Mathematics and Statistics, Changchun University of Science and Technology. She works on underwater image processing.